Plasmons: Chemical Bonding Coupling Induced Surface Plasmon Resonance Splitting in Self-Assembled Gold Nanoparticles

Yen Hsun Su

Department of Physics, National Cheng Kung University, Tainan 70101, Taiwan

Shih-Hui Chang*

Institute of Electro-Optical Science and Engineering, National Cheng Kung University, Tainan 70101, Taiwan

Lay Gaik Teoh

Department of Mechanical Engineering, National Pingtung University of Science and Technology, Pingtung 91201, Taiwan

Wen-Huei Chu

Department of Materials Science and Engineering, National Cheng Kung University, Tainan 70101, Taiwan

Sheng-Lung Tu

Center for Micro/Nano Science and Technology, National Cheng Kung University, Tainan 70101, Taiwan

Received: August 25, 2008; Revised Manuscript Received: November 19, 2008

Recently, the effect of π-bonding electrons conjugating to a gold surface has been predicated by first principles. In this paper, we observe surface plasmon resonance splitting due to the covalence and π-bonding electrons conjugated effect. When surfactantless Au NPs are linked on the glass substrate by sulfur, the SPR peak is split from one mode (638 nm) into two modes at 615 and 643 nm. The binding energy of 3s electrons for sulfur atoms has a huge red-shift in XPS peaks to confirm the π-bonding electrons conjugated effect. Furthermore, a proposed classical coupling dielectric function model, adding the gold−sulfur covalence bonding effect and conjugated π-bond electrons from sulfur to gold into the Drude model, is achieved to explain the mechanism of the SPR split phenomenon. In the extreme case, when the Au surface atoms are all covered by thiol sulfur atoms, or not covered at all by thiols, the SPR peak will not split. We found 3.28% of the Au atoms are bound by sulfur atoms and 92% of the conjugated electrons of the sulfur atoms transfer to Au electronic gas. The coverage rate of the sulfur atoms bonded to the surface of the Au atoms is about 25%, and this can cause the SPR splitting.

1. Introduction

Metal nanoparticles are of great interest because of their unique electronic, optical, and magnetic properties.[1−5] For example, nanoparticles of noble metals, such as gold and silver, have attracted much attention[6−8] because of their color variations in the visible region. Their rich optical properties are based on plasmon resonance, which is due to the collective oscillation of the electrons at the surface of the nanoparticles.[9−11] Gold nanoparticles (Au NPs) are a major research area in the field of unusual chemical and physical properties, with potential uses as catalysts, novel electronics, solar cells, and biosensors.[1−11]

Some functional groups of organic molecules, such as the mercapto-group with high affinity, are expected to modify the surface of Au NPs.[12−14] Thiol ligands bond to gold strongly due to the covalent bond between Au and sulfate.[13] The appearance of molecular linkers raises an interesting issue, as self-assembly monolayer (SAM) will change the optical and electric characteristics of the Au interface. Some first principle calculations[15−19] report that the π-bonding of a molecular linker can conjugate electrons to the surface of gold. However, the behavior of π-bonding conjugation is difficult to observe directly in experiments, and thus in this study, we focus on the interaction of covalence and π-bonding conjugation between gold and sulfur by observing the surface plasmon resonance (SPR) spectrum. Subsequently, a classical coupling dielectric function model is used to confirm our results.

In this paper, we investigate the influence of the chemical bonding for sulfur on surfactantless gold NPs with the use of SPR. In the sample preparation, surfactantless Au NPs are used to avoid any chemical bonding effect on the NPs surface. Surfactantless Au NPs are then adsorbed on the glass substrate by the evaporating and self-assembly methods. Notably we find that the SPR peak splits into two modes when a surfactantless Au NP interacts with thiols on the substrate. One of the SPR peaks is red-shifted, and the other is blue-shifted and considerably narrower. The splitting of SPR peaks is due to two different kinds of chemical bonding between Au and S, one is the covalent bond and the other is the π bond. We found the covalent bond between sulfur and gold atoms causes the SPR peak red-shift, while the π-bonding effect between the sulfur and gold atoms results in the blue-shift. This observation was

* To whom correspondence should be addressed. Tel.: (886) 2757575 ext. 6529. Fax: (886) 62747995. E-mail: gilbert@mail.ncku.edu.tw.

10.1021/jp807584h CCC: $40.75
Published on Web 02/16/2009

not anticipated on the basis of earlier work on the surface and local plasmonics cases. We propose a simple classical coupling dielectric function model, adding the covalence bonding and conjugated π-bond effect into the Drude model, in order to explain the mechanism of the SPR split phenomenon. Some first principle calculations[15−17] validate our assumption of charge transfer from sulfur to the Au surface, and we expect that this SPR splitting phenomenon has potential applications in the fields of biosensing, bioimaging, nanophotonics, and quantum information.

2. Experimental Section

Preparation of Au NPs. Au NPs were deposited by a chemical-reduction method using Au salt and $NaBH_4$ (Alfa Aesar Chemical Co.) solution. $NaBH_4$ in tretrahydrofuran (THF) and $HAuCl_4$ (Alfa Aesar Chemical Co.) in THF were mixed at room temperature with vigorous stirring. The mole ratio of $NaBH_4$ and $HAuCl_4$ was 10:1. A low concentration of Au NPs, 0.5 μM $HAuCl_4$ in THF, was synthesized in order to prevent Au NPs from aggregating. The color of the solution turned from yellow to black. Surfactant-less Au NPs were synthesized in THF.

Fabrication of Surfactantless Au NPs on the Glass Substrate by an Evaporating Method. The glass substrate sits at the bottom of the beaker, and 20 mL of 0.5 μM $HAuCl_4$ in THF is injected into the beaker. The beaker is left still for 36 h so that the THF evaporates, and Au NPs are deposited on the glass substrate. Subsequently, water is used to wash the sample to remove NPs which do not physically adsorb on the substrate.

Modification of Surfactantless Au NPs on the Glass Substrate by a Self-Assembly Method. Mercapto-propyl-trimethoxy-silane (MPTMS) (Alfa Aesar Chemical Co.) is used as a molecular linker connecting the substrate with Au NPs by a self-assembly monolayer process. A total of 1.5 mL of 10% MPTMS in THF is baked dry on the glass substrate as a molecular linker on which Au NPs are modified. The substrate is then immersed in Au colloid for 36 h to make modified Au NPs on the surface. The linking of Au NPs on the sulfur of MPTMS and the aggregation of additional Au NPs on linked NPs happens after 36 h via the self-assembly method. After NPs link on the sulfur of MPTMS for 36 h, the samples are taken out and washed with ethanol and then water in order to remove the additional NPs which do not link to the sulfur of MPTMS.

Instruments and Measurements. The morphologies of surfactantless Au NPs were observed by TEM. Surfactantless Au NPs colloid is dipped on the grid. The as-grown product is observed with a Hitachi model HF-2000 transmission electron microscope operating at 200 kV. The absorption of surfactantless Au NPs is observed with the UV−vis spectrum (Hitachi U-2001 spectrophotometer), and the sample is directly injected into a quartz tube for analysis. Au NPs on the glass substrate are observed by atomic force microscopy (AFM) and Cytoviva OM. The ellipsometric spectra are in the range of visible light. The optical properties and thickness with ellipsometry are detected or fitted via ellipsometry (h-VASE, J. A. Woollam. Co., Inc.), and X-ray photoelectron spectroscopy (XPS) is used to measure the binding energy of f electrons for Au atoms and s electrons for sulfur atoms.

3. Results and Discussion

3.1. Characteristics of Surfactantless Au NPs in THF. The shape of the Au NPs in THF is close to sphere-like, and they aggregate together after dropping on the grid, as shown in Figure 1a. The average size of the Au NPs is about 10 nm. Since no ligands or surfactants were added, nanoparticles must be prepared in a very low concentration to avoid collision-induced aggregation. Furthermore, tetrahydrofuran (THF) is a molecule with both hydrophilic and hydrophobic ends, which further prevents the aggregation. Hence, the lifetime of Au NPs colloid in THF solution is longer than the sample preparation time.

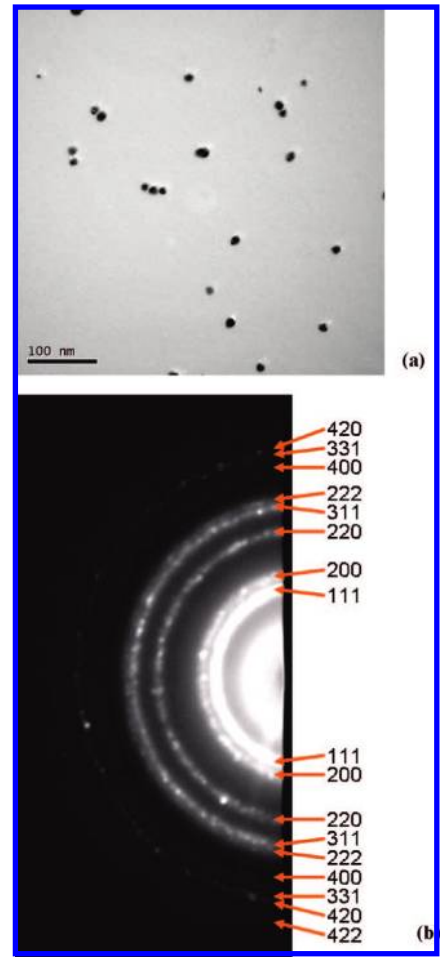

Figure 1. (a) TEM image and (b) diffraction pattern of the Au NPs in THF.

The electron diffraction pattern of Au NPs shown in Figure 1b is the standard indexed diffraction pattern for a face center cubic (FCC) crystal (JCPDS-ICDD 02−1095, $a = b = c =$ 4.068 Å). From the absorption spectra, the measured surface plasmon resonance of Au NP in THF is peaked at 563 nm. The extinction spectrum calculated by Mie theory for a 10 nm Au NP in $n = 1.4$ medium also indicates a SPR peak at 562 nm, as shown in Figure 2.

3.2. Characteritics of Au NPs on Glass Substrate by Evaporation and Self-Assembly Methods. The morphology of Au NPs on the glass substrate is obtained by AFM. The Au NPs are fabricated on the substrate by an evaporation method, as shown in Figure 3a, whereas Figure 3b shows the morphology produced by a self-assembly MPTMS method. From the AFM images, random distribution is observed for the morphology of Au NPs on the glass substrate produced by both the evaporating and self-assembly methods.

Dark-field spectroscopic images of the Au NPs produced by the evaporating and self-assembly methods on the glass substrate are shown in Figure 4, panels a and b, respectively. When panels a with b in Figure 4 are compared, the scattering light of Au

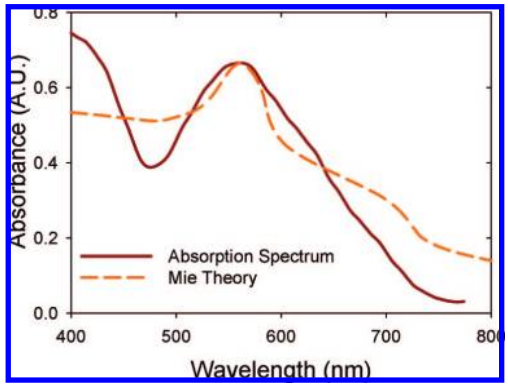

Figure 2. UV−vis spectrum of the Au NPs in THF.

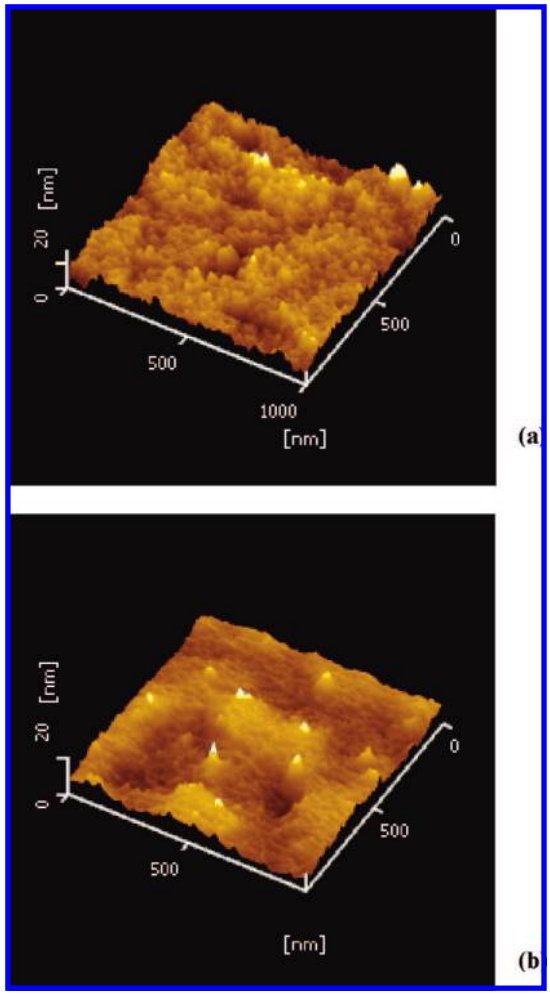

Figure 3. AFM images of the Au NPs and air composite layer produced on the glass substrate (a) by the evaporating method and (b) by the self-assembly method.

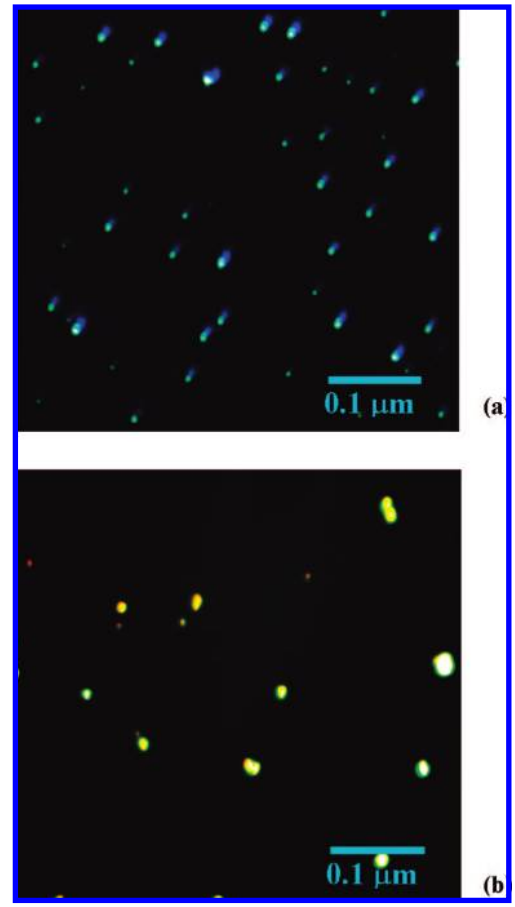

Figure 4. Dark-field spectroscopic image of the Au NPs produced on the glass substrate (a) by the evaporating method and (b) by the self-assembly method.

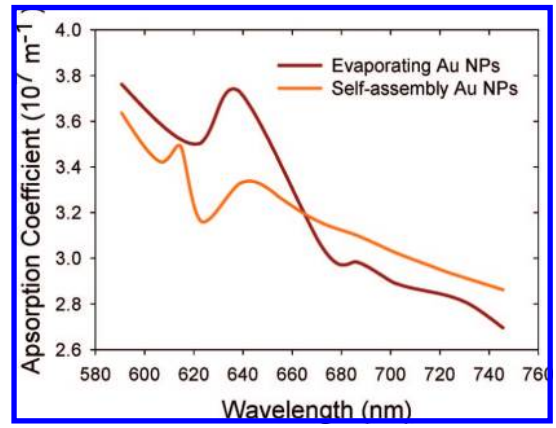

Figure 5. Extinction coefficients of the Au NPs produced on the glass substrate by the evaporating method and by the self-assembly method.

NPs produced by the evaporating method on the glass substrate is different from that for these obtained by the self-assembly method. The scattering light associated with the evaporating method is green-blue in Figure 4a, whereas that associated with the self-assembly method is yellow-orange color in Figure 4b. Figures 3 and 4 show Au NPs were randomly spread on the surface of the glass substrate, and Wei et al.[20] also report random distribution of Au NPs on glass substrate when 3−5 nm gold nanoparticles are linked on sulfur of MPTMS. Fractal structures of Au NPs due to aggregation effect were not observed.

The extinction spectra of Au NPs on the substrate produced by the evaporating case are shown as the red line in Figure 5, and the absorption peak of the surfactantless Au NPs is at 638 nm. When the Au NPs are linked on the substrate by the self-assembly method, the absorption spectrum is shown as the yellow line in Figure 5, and SPR peaks are centered at 643 and 614 nm. Sherry et al.[21] report the splitting of the SPR mode in Ag nanocubes[21] due to the substrate effect produced by the asymmetric dielectric environment experienced by special Au nanostructures, such as nanocubes and nanosea-urchins.[22] For the top interface, the special Au nanostructure is in contact with air, whereas for the bottom interface, it is in contact with the substrate. Because of the interaction of the surface plasmon mode with the substrate, the SPR peaks split into two modes.[21,22]

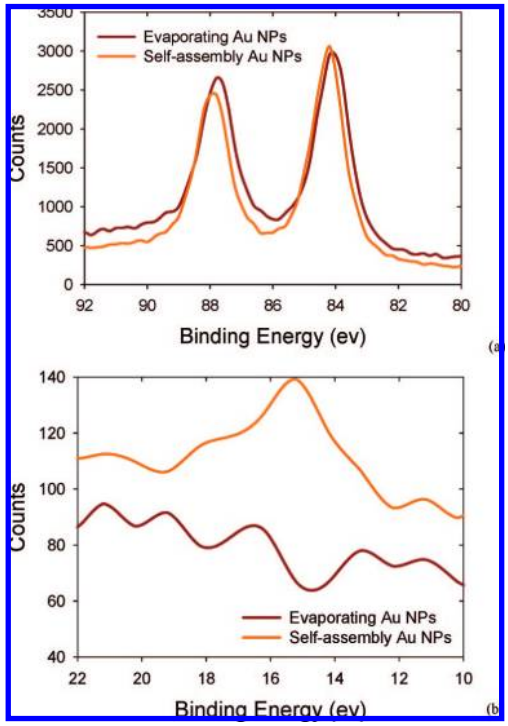

Figure 6. XPS spectrum for (a) 4f and (b) low energy of the Au NPs on the glass substrate for the evaporating method and the self-assembly method.

However, for Au spherical nanoparticles, the field distribution of the SPR mode is beside the gold nanoparticle, not in the substrate.[21] SPR of Au spherical nanoparticle does not split into two modes.

XPSs of the Au NPs are shown in Figure 6. When Au does not bond to any chemicals, the binding energies of $4f_{7/2}$ and $4f_{5/2}$ electrons for Au are 84 and 88 eV, respectively.[23] When Au bonds with some chemicals, the binding energies of $4f_{7/2}$ and $4f_{5/2}$ electrons are blue-shifted. Specifically, the binding energy of $4f_{7/2}$ electrons usually blue-shifts from 84 eV to 84∼85.5 eV.[23]

For the evaporating case, $4f_{7/2}$ is unchanged at 84 eV. For the self-assembly case, when the Au NPs bond with sulfur, the binding energy of $4f_{7/2}$ electrons is blue-shifted to 84.3 eV, and the binding energy of $4f_{5/2}$ electrons is also blue-shifted. This indicates the electron density of Au will be affected by the sulfur bonding.

When sulfur does not bond with any chemicals, the binding energy of 3s electrons of sulfur is at 18 eV. In Figure 6b, the binding energy of 3s electrons for sulfur to Au is red-shifted from 18 to 15.2 eV, which is a huge shift in XPS peaks. In the other words, the binding energy of 3s electrons for sulfur is lower than that of nonbonding sulfur. Heimel et al.[15−17] report that the π-bonding electrons of the sulfur linker are able to conjugate to the surface of a noble metal, such as Au NPs. Consequently, we do observe a huge red shift in the XPS peak of sulfur atoms linking on Au NPs.

3.3. Model of Coupled Dielectric Function. From our measurement, the SPR frequency ω_{sp} of Au NPs is at 635nm (1.95 eV) for the evaporating case. By electrostatic approximation,[24] ω_{sp} is given by

$$\omega_{sp} = \frac{\omega_p}{\sqrt{1+A}}$$

According to the geometrical effect, $A = 2$ for spherical metal,[25] the plasma frequency ω_p is at 3.38 eV. By definition, the plasma frequency occurs at $\varepsilon(\omega) = 0$. The dielectric function ε_m for the evaporating case is

$$\varepsilon_m(\omega) = 1 + \frac{N_f e^2}{m\varepsilon_0}\frac{1}{-\omega^2 + i\omega\gamma}$$

where N_f is the number density of free electrons and is related to ω_p as $\omega_p = (N_f e^2)/(m\varepsilon_0)$. Thus, the dielectric function of Au NPs for the evaporating case will cross the zero point at 3.38 eV.

On the other hand, the frequency ω_{sp} for the self-assembly case is measured at 610 and 643 nm. By electrostatic approximation, plasma frequency ω_p is split to 3.34 and 3.52 eV, and thus the dielectric function for the self-assembly case will cross the zero point at these two frequencies.

The dielectric function of Au NPs for the self-assembly case can be considered as a superposition between the dielectric function ε_m for surfactantless Au NPs and the chemical bonding ε_{chem}. There are two contributions to ε_{chem}. The electrons between the Au and S atoms can form (A) the covalent bond (Au−S), which binds some free electrons from Au NPs, and (B) the π-bonding conjugating effect, which contributes electrons to Au from the sulfate atoms, as shown in Scheme 1.

SCHEME 1: Au NPs Linked by MPTMS[a]

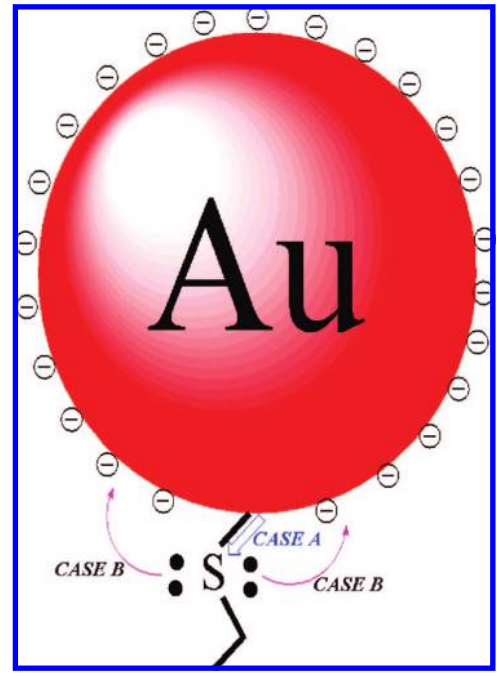

[a] Case A indicates the covalent bond between sulfur and gold atoms. Case B indicates the lone pairs of sulfur atoms which contribute electrons to Au NP.

In case A, each sulfur atom can contribute one electron to bind one electron of a Au atom to overlap a covalence bond. Hence, the first term of ε_{chem} is a Lorentz oscillator to describe the binding electron as follows:

$$\varepsilon_{chem}^{\text{covalence bonding}}(\omega) = \frac{N_b e^2}{m\varepsilon_0}\frac{1}{\omega_c^2 - \omega^2 + i\omega\gamma}$$

in which ω_c is the binding frequency of a covalence bond, N_b is the number density of covalent binding electrons.

In case B, when one electron of a sulfur atom binds with one electron of a Au atom, π-bonding electrons of the sulfur linker may conjugate to gold atom.[15−17] Consequently, the

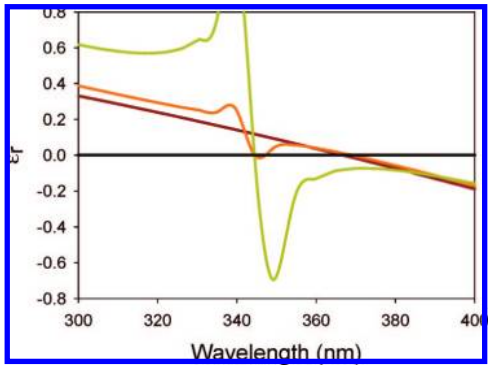

Figure 7. Simulation of coupling dielectric function for Au NPs. (Red line: $N_b/N_f = 0$; origin line: $N_b/N_f = 3.28\%$, $x = 92\%$; yellow line: $N_b/N_f = 13\%$, $x = 88\%$.)

π-bonding electrons of sulfur will red-shift.[23] Therefore, the second term of ϵ_{chem} is a Lorentz oscillator to describe conjugated π-bonding electrons.

$$\varepsilon_{chem}^{\text{Pi bonding}}(\omega) = \frac{(xN_b - N_b)e^2}{m\varepsilon_0} \frac{1}{\omega_\pi{}^2 - \omega^2 + i\omega\gamma}$$

in which x is the portion of conjugative bonding electrons which are support by the sulfur linker. ω_π is the binding frequency of a conjugated π-bond.

The dielectric function due to both the chemical covalent and π-bonding can be expressed as

$$\varepsilon_{chem}(\omega) = \frac{N_b e^2}{m\varepsilon_0} \frac{1}{\omega_c{}^2 - \omega^2 + i\omega\gamma} + (x-1)\frac{N_b e^2}{m\varepsilon_0} \frac{1}{\omega_\pi{}^2 - \omega^2 + i\omega\gamma}$$

The overall dielectric function $\varepsilon_{coupling}$ of Au NPs in the self-assembly case is a combination of ε_m and ε_{chem}

$$\varepsilon_{coupling}(\omega) = \varepsilon_m(\omega) + \varepsilon_{chem}(\omega)$$

Therefore

$$\varepsilon_{coupling}(\omega) = 1 + \frac{N_f e^2}{m\varepsilon_0} \frac{1}{-\omega^2 + i\omega\gamma} + \frac{N_b e^2}{m\varepsilon_0} \frac{1}{\omega_c{}^2 - \omega^2 + i\omega\gamma} + (x-1)\frac{N_b e^2}{m\varepsilon_0} \frac{1}{\omega_\pi{}^2 - \omega^2 + i\omega\gamma}$$

The coupling dielectric function is shown in Figure 7.

3.4. Comparison of the Coupling Dielectric Function Model and the Experimental Data. For the above results, the plasma frequency ω_p for surfactantless Au NPs is at 3.38 eV (367 nm). In the self-assembly case, the plasma frequency ω_p for the coupling dielectric function is split to 3.34 eV (371 nm) and 3.58 eV (346 nm). By fitting the experimental data with the proposed model of $\varepsilon_{coupling}$, when the ratio between N_b and N_f is 0.0328 and x is 0.92, the coupling dielectric function will cross zero at 3.34 and 3.58 eV, as shown in Figure 7. 3.28% of the free electrons of the Au atoms are bound by the sulfur atoms, and 92% conjunctive electrons transform to Au electronic gas for each sulfur atom which has two lone pairs.

For a 10-nm Au nanoparticles, there are about 31 000 atoms, each of which donates one 6s electron, forming the free electron sea. Because the ratio of N_b and N_f is 0.0328, about 1017 free electrons are bond by the sulfur. Each nanoparticle can bond with 1017 thiols, and 92% of sulfur lone pair electrons conjugate to Au free electrons. Therefore, about 936 electrons are contributed by sulfur (thiol) immobilized on the glass substrate.

The percentage of surface atoms for 10-nm Au spherical NPs is about 13%, estimated by Molder et. al.[26] The coverage rate of sulfur bonded surface Au atoms is about 25%.

In the extreme case, when the Au surface atoms are all covered by thiol sulfur atoms ($N_b/N_f = 13\%$, $x = 92\%$), the coupling dielectric function $\varepsilon_{coupling}$ will cross zero at 3.60 eV (344 nm). According to the electrostatic approximation, ω_{sp} is about 2.08 eV (~597 nm). The coupling dielectric function will cross zero at only one point, as shown in the yellow line in Figure 7.

In either case, when the surface is all covered, or not covered at all by thiols, the coupling dielectric function $\varepsilon_{coupling}$ cross zero at only one point.

When the surface is covered with some thiols, π-bonding electrons of the sulfur linker conjugate to gold atoms. The coupling dielectric function crosses zero at two points, and thus the SPR peak will be split into two modes.

Finally, the red-shifted peak at 643 nm is broader than one at 635 nm in Figure 5 because covalent bonding increases the electron damping of SPR. The blue-shifted peak at 615 nm is narrower than one at 635 nm in Figure 5 because the conjugating electrons reduce the electron damping of SPR. The above results show the great influence of SPR due to the presence of sulfur atoms brought about by the self-assembly method.

4. Conclusions

In this paper, we observe surface plasmon resonance splitting due to the covalence and π-bonding electrons conjugating effect. In the evaporating case, the SPR peak of surfactantless Au NPs is at 635 nm. In the self-assembly case, the SPR peaks of Au NP electrons red-shift to 643 nm and blue-shift to 615 nm. XPS measurements observed a huge red-shift for the binding energy of 3s electrons in sulfur atoms, which confirm the π-bonding electrons conjugating effect. Furthermore a proposed classical coupling dielectric function model, adding the gold−sulfur covalence bonding effect and the conjugated π-bond electrons from sulfur to gold into the Drude model, is developed to explain the mechanism of the SPR split phenomenon. We found 3.28% of the Au atoms are bound by sulfur atoms and 92% of conjugated electrons of the sulfur atom transfer to Au electronic gas. The coverage rate of sulfur atoms bonded to surface Au atoms is about 25%. In the extreme case, when the Au surface atoms are all covered, or not covered at all by thiols, the SPR peak will not split due to the prediction of the classical coupling dielectric function model. When the surface is covered with some thiols, π-bonding electrons of the sulfur linker conjugate to gold atoms, and the SPR peak will split into two modes. We believe this work provides an important insight into the influence of SPR on Au NPs due to the presence of the molecular linker. This phenomenon has potential applications in the fields of biosensing, bioimaging, nanophotonics, and quantum information.

Acknowledgment. This work was financially supported by the National Science Council of Taiwan, the Republic of China, Grant No. NSC 96-2628-M-006-001-MY3, which is gratefully acknowledged. The authors also thank the National Center of Theoretical Sciences (NCTS) and Y. K. Wu in Taiwan.

References and Notes

(1) Sherry, L. J.; Chang, S.-H.; Schatz, G. C.; Duyne, R. P. V.; Wiley, B. J.; Xia, Y. *Nano Lett.* **2005**, *5*, 2034.

(2) Kwak, E.-S.; Henzie, J.; Chang, S.-H.; Gray, S. K.; Schatz, G. C.; Odom, T. W. *Nano Lett.* **2005**, *5*, 1963.
(3) Shuford, K. L.; Lee, J.; Odom, T. W.; Schatz, G. C. *J. Phys. Chem. C* **2008**, *112*, 6662.
(4) Yu, K. F.; Kelly, K. L.; Sakai, N.; Tatsuma, T. *Langmuir* **2008**, *24*, 5849.
(5) Kelly, K. L.; Yamashita, K. *J. Phys. Chem. B* **2006**, *110*, 7743.
(6) Anker, J. N.; Hall, W. P.; Lyandres, O.; Shah, N. C.; Zhao, J.; Van Duyne, R. P. *Nat. Mater.* **2008**, *7*, 442.
(7) Jensen, L.; Zhao, L.; Schatz, G. C. *J. Phys. Chem. C* **2007**, *111*, 4756.
(8) Reilly, T., III.; Chang, S.-H.; Corbman, J. D.; Schatz, G. C.; Rowlen, K. L. *J. Phys. Chem. C* **2007**, *111*, 1689.
(9) Montgomery, J. M.; Gray, S. K. *Phys. Rev. B* **2008**, *77*, 125407.
(10) Ritchie, R. H.; Eldridge, H. B. *Phys. Rev.* **1962**, *126*, 1947.
(11) Liu, G. L.; Long, Y.-T.; Choi, Y; Kang, T.; Lee, L. P. *Nat. Method* **2007**, *4*, 1015.
(12) Sun, L.; Crooks, R. M.; Chechik, V. *Chem. Commun.* **2001**, 359.
(13) Brust, M.; Fink, J.; Bethell, D.; Schiffrin, D. J.; Kiely, C. J. *J. Chem. Soc. Chem. Commun.* **1995**, *16*, 1655.
(14) Daniel, M.-C.; Astruc, D. *Chem. Rev.* **2004**, *104*, 293.
(15) Heimel, G.; Romaner, L.; Brédas, J. L.; Zojer, E. *Phys. Rev. Lett.* **2006**, *96*, 19–196806.
(16) Heimel, G.; Romaner, L.; Brédas, J. L.; Zojer, E. *Surf. Sci.* **2006**, *600*, 19–4548.
(17) Heimel, G.; Romaner, L.; Brédas, J. L.; Zojer, E. *Nano Lett.* **2007**, *7*, 932.
(18) Zhu, M.; Aikens, C. M.; Hollander, F. J.; Schatz, G. C.; Jin, R. *J. Am. Chem. Soc.* **2008**, *130*, 5883.
(19) Heimel, G.; Romaner, L.; Brédas, J. L.; Zojer, E. *Acc. Chem. Res.* **2008**, *41*, 721.
(20) Wei, Z.; Zamborini, F. P. *Langmuir* **2004**, *20*, 11301.
(21) Sherry, L. J.; Chang, S.-H.; Schatz, G. C.; Duyne, R. P. V.; Wiley, B. J.; Xia, Y *Nano Lett.* **2005**, *5*, 2034.
(22) Su, Y. H.; Lai, W. H.; Chen, W.-Y.; Hon, M. H.; Chang, S.-H. *Appl. Phys. Lett.* **2007**, *90*, 101905.
(23) Moulder, J. F. *Handbook of X-ray Photoelectron Spectroscopy*; Physical Electronics, Inc.: Eden Prairie, MN, 1995.
(24) Barber, P. W.; Chang, R. K. *Optical Effects Associated With Small Particles*; World Scientific Publishing Co., Inc.: Singapore, 1988.
(25) Kreibig, U.; Vollmer, M. *Optical Properties of Metal Clusters*; Springer-Verlag: Berlin, 1995.
(26) Buffat, H.; Borel, J. P. *Phys. Rev. A* **1976**, *13*, 2287.

JP807584H